Original Article

Wearable Wireless Sensors for Measuring Calorie Consumption

Faranak Fotouhi-Ghazvini, Saedeh Abbaspour

Department of Computer Engineering and IT, Faculty of Engineering, University of Qom, Iran

Abstract

Background: The tracking devices could help measuring the heart rate and energy expenditure and recognizing the user's activity. The calorie measurement is a significant achievement for the fitness tracking and the continuous health monitoring. **Methods:** In this paper, a combination of an accelerometer and a photoplethysmography (PPG) sensor is implemented to calculate the calories consumed. These sensors were mounted next to each other and then were placed on the ankle and finger by flat cable. The sensed data are transferred via Bluetooth to a smartphone in a serial and real-time manner. An Android App is designed to display the user's health data. The average amount of consumed energy is obtained from the combination of the accelerometer sensor based on the laws of motion and the PPG sensor based on the heart rate data. **Results:** The designed system is tested on 10 nonathlete males and 10 nonathlete females randomly. By applying the wavelet, the value of the acceleration signal variance was reduced from 3.2 to 0.8. The correlation between PPG and pulse oximeter was 0.9. Moreover, the correlation of the accelerometer and treadmill was 0.9. The root mean square error (RMSE) and the *P* value of the calorie output from PPG and pulse oximeter are 0.53 and 0.008, respectively. The RMSE and the *P* value of the calories output from the accelerometer and the treadmill are 0.42 and 0.007, respectively. **Conclusion:** Our device validity and reliability were good by comparing it with a typical smart band, smart watch, and smartphone available in the market. The combined PPG and the accelerometer sensors were compared with the gold standard, the pulse oximeter, and the treadmill. According to the results, there is no significant difference in the values obtained. Therefore, a mobile system is augmented with the wireless accelerometer and PPG that are connected to a smartphone. The system could be carried out with the user at any time and any place.

Keywords: *Accelerometer, activity monitoring, calorie consumption, photoplethysmography, smartphone health application*

Submitted: 08-Apr-18 **Revision:** 08-May-18 **Accepted:** 05-Dec-19 **Published:** 06-Feb-20

Introduction

The recent advances in manufacturing mobile devices and the rise of wearable sensors embedded in people's everyday lives have led to the concept of mobile healthcare (mHealth) monitoring. The mHealth is defined as access and practice of healthcare through mobile telecommunication, multimedia technology, and wireless body sensors through a smartphone healthcare application (App).[1] The healthcare Apps include (i) fitness, diet, and nutrition Apps and (ii) disease and treatment management Apps. According to Gartner, 40% of digital health systems in 2021 will shift to wearable which 90% will include fitness trackers.[2] These mHealth Apps could calculate the amount of energy consumed during a physical activity using accelerometers,[3] gyroscope,[3] and GPS[2,4-6] to obtain and analyze the required data. Hwang *et al*. provided a fitness system embedded in shoes to measure steps, calorie, and biomedical information using the pressure sensors.[7] Adi *et al*. have built a system to measure the heart rate, electrocardiogram (ECG) signal, step count, and calorie consumption using the smartphone's accelerometer.[8] Pande *et al*. used smartphone's sensors such as accelerometer and barometer to obtain the energy expenditure.[9] Pal and Hepsiba estimated the user's energy expenditure using the smartphone's accelerometer and GPS.[10] Duclos *et al*. have used accelerometer data to measure the energy expenditure.[11] Li *et al*. used the ECG and accelerometer sensors to estimate the energy expenditure.[12] Altini *et al*. used five

How to cite this article: Fotouhi-Ghazvini F, Abbaspour S. Wearable wireless sensors for measuring calorie consumption. J Med Signals Sens 2020;10:19-34.

Address for correspondence:
Dr. Faranak Fotouhi-Ghazvini, Department of Computer Engineering and IT, Faculty of Engineering, University of Qom, Alghadir Boulevard, The Old Isfahan Road, Qom, Iran.
E-mail: f-fotouhi@qom.ac.ir

Access this article online

Website: www.jmssjournal.net

DOI: 10.4103/jmss.JMSS_15_18

Quick Response Code:

accelerometer sensors attached to the body to assess the energy expenditure during the daily activities.[13] Carneiro *et al*. used a smartphone's accelerometer to estimate the energy expenditure.[14] Majority of these projects rely on smartphone-embedded sensors to collect the physiological data, which hugely lack precision and accuracy. On the other hand, there are many smart band devices in the market such as Fitbit, Fitbit Flex, Fitbit Zip, and Garmin equipped with wireless sensors that measure the fitness parameters during the daily life. In the study by Boman and Sanches,[15] the Fitbit accelerometer utilized the user's weight and the stride length during daily activity. In the study by Duus *et al.*,[16] the Fitbit was incorporated to increase the activity level; however, it ignored to differentiate between different activities. In the study by Asimina *et al.*,[17] the Fitbit was joint with a smartphone app for step count, but it wrongly underestimated the step counts. In the study by Camp and Hayes,[18] the Fitbit was incorporated to measure the step counts though it was imprecise. In addition to the smart bands, the smart watches with fitness-monitoring capabilities are available. Similarly, in the smart watch market, for instance, in the studies by Schneider and Chau[19] and Hamari *et al.*,[20] the ActiGraph was used which erroneously overestimated the frequency of the activity and the step counts. The Huawei and Apple watches include an accelerometer, gyroscope, heart rate, altimeter, and microphone sensors.[21] In the study by King and Sarrafzadeh,[22] the basic B1 smart watch was incorporated for dementia care at home. It provided the heart rate, the ambient temperature, and the activity levels. However, it did not reveal the number of calories consumed during the daily activities. In the study by Boletsis *et al.*,[22] the gold standard was not considered to compare the activity measurements. In the study by Bojanovsky *et al.*,[23] the detection of fall and seizure was carried out with the smartphone and smart watch for people with epilepsy. The smart watch output was used along with the decision tree algorithm with accuracy between 89.7% and 98.5%. In paper,[24] the environment was adapted for older adults dynamically adapting the through smart watch-based mood detection. However, the mood detection was not accurately recognized.

Table 1 compares the four different fitness devices with our proposed device. The device with its accompanied Apps will be introduced in the following sections. According to Table 1, neither of these devices differentiates between activities. For example, it is not evident during an activity if a person with a specific step count was running, walking, or swimming. Therefore, the Apps cannot be customized to track and monitor disease and aid in treatment management.

Moreover, the step count and the heart rate frequency in the majority of these projects were not measured correctly, and the accurate readings were obtained only in sedentary position.[7,24] All of these devices come with an elaborated smartphone App; however, they do not provide an open-source platform for developers, engineers, and scientist. Therefore, their customization ability is minimal. When considering the cost, these fitness trackers and smart watches are much more expensive than the device implemented in the present project.

In this research, we aim to present a kit that is composed of accelerometer and photoplethysmography (PPG) sensors to measure the amount of energy consumed during physical activity. The accelerometer is suitable for measuring the physical activity and the energy consumed in different situations, including walking and going up the stairs. According to Figure 1, this device can be connected to smartphone's via Bluetooth and all the received information is stored in a database utilizing sensors and are retrievable for subsequent reference. The data are then transmitted to the doctor/nurse and stored in the central system for subsequent actions. Following the analysis of the data received by the doctor/nurse, appropriate feedback is sent back to the user.

The article is organized as follows. In "Methods Section," the design of the PPG, the accelerometer sensors, and the mHealth App are introduced. In "Experimental Design Section," the experimental design explains how the PPG and the accelerometer sensors are calibrated and filtered. It also describes how the calorie consumption is calculated based on the heart rate and the accelerometer. "Results Section" presents the experiment results, by defining the population under the experiment and the formulas used for statistical analysis. It then compares the proposed device with the commercial devices. Next, our proposed kit was evaluated against gold standards. The gold standards in this research refer to the benchmark devices such as pulse oximeter and

Table 1: The comparison between the four commercial fitness devices with the proposed device

Features measured	Fitbit Flex2 band	Garmin Vivifit with a heart monitor	Huawei Watch 2	Apple Watch series 3 with GPS	Proposed device
Step count	✓	✓	✓	✓	✓
Heart rate count	✓	✓	✓	✓	✓
Accuracy during a motion activity	–	–	–	–	✓
Differentiating between activities	–	–	–	–	✓
Open source platform	–	–	–	–	✓
Price ($)	59.95[25]	199.00[26]	224.99[27]	749[28]	120

✓ – Global positioning system

treadmill that most accurately measure the number of heart rate, the number of steps, and the calorie consumption. The correlation of calorie consumption in PPG/pulse oximeter and accelerometer/treadmill is calculated. Subsequently, the calorie consumption is measured with PPG and accelerometer sensors considering the effect of the gender, weight, and age. In "Discussion Section," a discussion on the result is presented. In "Conclusion Section," the article is concluded.

Methods

In the previous research, the accelerometer and the heart rate sensors are separately implemented to determine the energy consumption during the physical activity. Typically, the sensors are embedded in smartphones or placed on a separate electronic board mounted on the human body. In our design, both sensors are installed on a single electronic board to provide a fitness kit, as shown in Figure 2. The acceleration data include the three dimensions of X, Y, and Z, while the PPG transmits analog data. The designed board uses Atmega32A microcontroller and Sim800 module to transmit the acceleration and the heart rate data that stored on a memory card. Coding is performed in Arduino software (Microchip Technology Inc, Chandler, Arizona, US), and the data are ultimately displayed on the user's smartphone. A lithium-ion battery, capable of lasting for 6 h, is used as a power supply for the device. Since the battery is lightweight, the board can be easily mounted on the user's body. The device size is 10 cm × 10 cm × 1.5 cm in length, width, and height, respectively. Its weight is about 200 g. The dimensions could be reduced to make it compatible with daily activities. The proposed device in its two layers' printed circuit board configuration costs about 60$, weighing about 120 g with the reduced size of 10 cm × 5 cm × 1.5 cm in length, width, and height, respectively. The device is attached on the ankle; the heart rate data are received using a flat cable connected to the PPG transreceiver placed on the finger. Figure 2 shows the designed circuit.

Photoplethysmography sensor

The PPG sensor is used to measure the heart rate by taking advantage of an infrared (IR) transmitter and receiver. The heart consists of the two upper chambers (i.e., atria) and the two lower chambers (i.e., ventricles). The sympathetic and parasympathetic nervous system stimulates a small mass of cells called the sinoatrial node in the right upper chamber (atria) of the heart. The heart's electrical impulses start from this node and then down through the conduction pathways stimulating the atria and ventricles. This process forms the heart's pumping action which coordinates the contraction of the heart's chambers. Each heartbeat is due to each contraction of the ventricles. Each heartbeat is about 60–100 times a minute in normal resting condition. According to the heart's electrical function, the *P* wave shows the atrial depolarization [Figure 3]. The

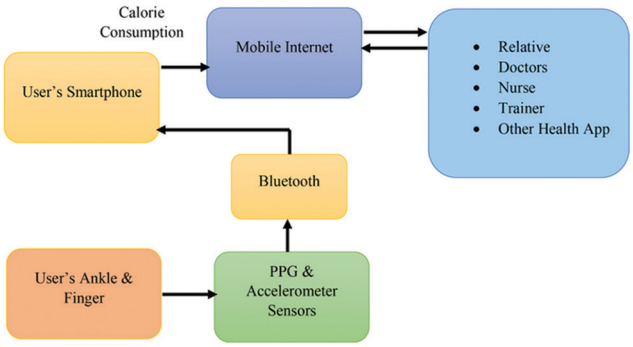

Figure 1: The interaction mechanism between the sensors and the user

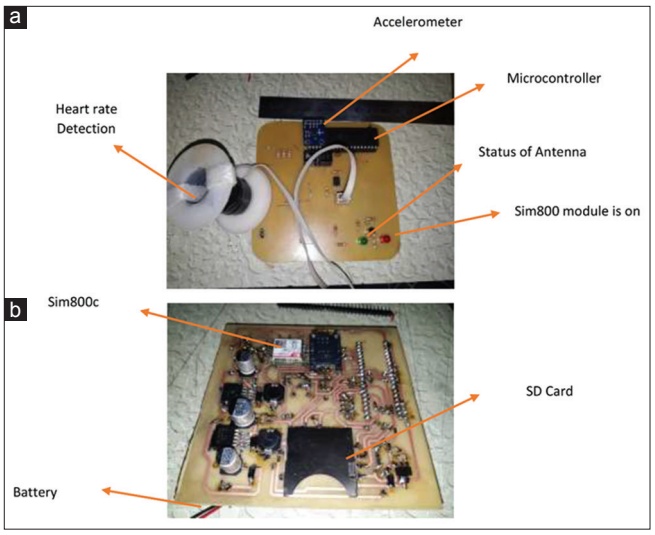

Figure 2: (a) Kit's front view, (b) kit's back view

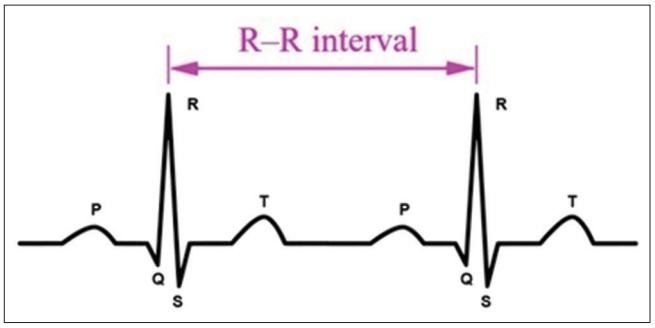

Figure 3: The electrocardiogram signal and its components

QRS complex represents the ventricular depolarization. The T wave is the ventricular repolarization. The R-peak represents a heartbeat and is the most prominent part of an ECG signal. The detected R-peaks represent the heart rate.

When individual places his/her finger between the IR transmitter and the receiver, the IR rays are transmitted and reflected from the skin. The sensor outputs the serial data which can be used to measure the heart rate. The reflected light represents the blood volume in the user's finger's vessel. A container with no light source holds the IR transmitter and receiver. It is connected to the board placed

on the ankle via a flat cable. Figure 4 illustrates how the heart rate frequency is categorized according to using the PPG according to.[29]

The PPG sensor consists of the following components:

1. An Atmega32 microcontroller
2. The LM358N integrated chip as a voltage amplifier
3. A memory module to store the heart rate data
4. An LED to display the heart rate by switching on and off for each beat
5. A 7.4 V lithium-ion battery.

Initially, the circuit outputs 1 V with a frequency response of 6 V with a cutoff frequency above 10 Hz. However, no output signal was detected on the oscilloscope when turning LED on or off. By applying an interface circuit, the output has improved and reached 5 V. The heart rate circuit required 5 V which was supplied by the regulator.

When the PPG sensor is mounted on the body and the person is carrying out an activity, the device may be affected by the environmental factors and produce inappropriate data. The physiological data need to be precise; therefore,

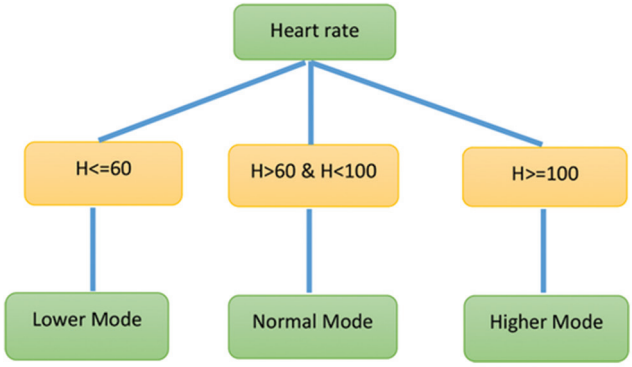

Figure 4: The heart rate categorization using threshold

the interface is used to output an improved PPG sensor signal. The block diagram in Figure 5 represents how the heart rate is extracted from the PPG sensor. When a finger is placed between the IR transmitter and receiver, the pulse is received by the first block, which amplifies and low-pass filters the signal. The LM358 is used to amplify the signal. The second block is our designated interface circuit that led to an improved outcome. The cut and saturation mode is present in this block by 0 V and 5 V output values, suitable for the microcontroller. The third block is complemented for signal processing in the Atmega32A microcontroller. The fourth block is related to control circuitry that includes a "Reset" and "Start" mode. The suitable output is displayed to the user via the LCD.

Novel photoplethysmography circuit improvement

An amplifier with eight pins and two states is used. If the voltage on the third pin is higher than that of the second, the output voltage equals +VCC volts; otherwise, the voltage equals −VCC volts. The comparison function with a diode IN4007 prevents negative voltage while allowing positive voltage to pass. However, the resulting voltage value is higher than 5 V. A series of a resistor and a Zener diode is used to limit the value of 5 V. Using this structure, only two voltage values (i.e., 0 V and 5 V) are generated as output for different input values. The Zener diode has a breakdown voltage of 5.5 V which prevents the circuit voltage from exceeding 5 V. The output signals can now be applied to the microcontroller. Further, depending on the type of programming, the microcontroller can be made sensitive to the low-to-high transition edge. The interface circuit has led to a suitable heart rate output. Power supply requirement for PPG circuit is 5 V, which is supplied through a 5 V regulator. Figure 6 is designed with the PSpice software (Electronics lab, USA). The numbering

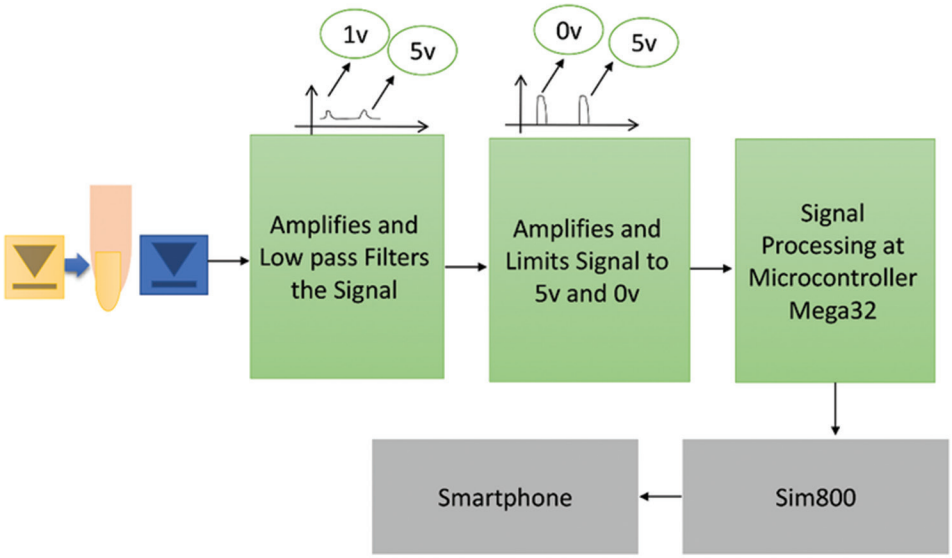

Figure 5: The block diagram of the photoplethysmography sensor

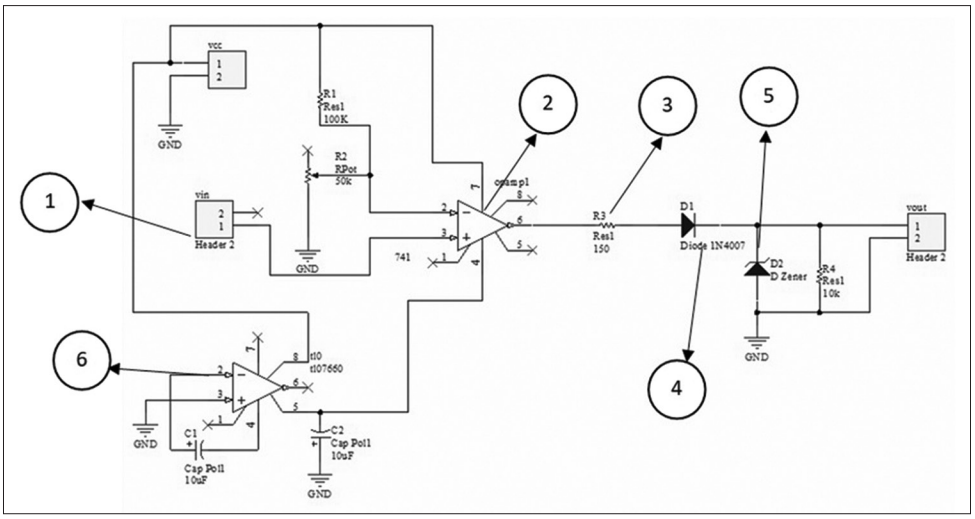

Figure 6: The heart rate circuit interface

system incorporated in Figure 5 can be explained as follows:

1. The input signal of heartbeat rate is measured after amplification
2. This IC has been converted to the comparator circuit. The input signal is instantaneously compared with the base-2 signal. Whenever the voltage level of the base-3 signal exceeds the base-2 signal, maximum feed voltage (around 9 V) is generated at the outlet of this IC, i.e., base 6. This voltage is not appropriate for applying to the microcontroller and shall be reduced to 5 V
3. At the base-6 of the IC, 9 V is generated. However, only 5 V is collected at terminals of Zener diode, and the rest of the voltage dissipates at the two terminals of 150 Ω resistor
4. This diode does not permit transmission of negative signals and only transmits the positive signals
5. The Zener diode is used for voltage stabilization and does not allow the potential difference at its two terminals to exceed the Zener's 5 V. The Zener voltage of this diode is 5 V which are suitable for applying to the microcontroller. The Zener diode is available with a voltage below or over 5 V, but only 5 V is required for the present circuit
6. The negative voltage generator is for the proper performance of the comparator IC.

Accelerometer

The accelerometer sensor provides an analog output representing acceleration on the three axes X, Y, and Z, one of which is the acceleration of gravity. Some designs use the vertical axis to detect the steps by claiming that acceleration is more distinct on the vertical axis.[30] However, other studies use all three axes for this purpose. Acceleration data are obtained at a sample rate of 32 Hz. The module's sensitivity for each axis is six bits allowing 2^6 of separation. Acceleration measurements range from −3 g to +3 g.[31] The module requires a voltage of 1.8–3.5 V and the regulator provides 3.3 V.

Mobile healthcare application navigation system

The sensors are mounted on the ankle and the data are transferred to an Android app on a smartphone via Bluetooth. The App's interface consists of five screens to carry out the turning on/off the Bluetooth, receiving the accelerometer and heart rate readings, and representing the calculated calorie. The App navigation system is shown in Figure 7. The rectangles used in Figure 7 represent java classes. Those classes implemented the components of the App to provide a suitable output of the heart rate and calories. The SQLite database is used to store the user data. To calculate the calories from the accelerometer, data Eq. (1) and Eq. (6) are used. Once the heart rate is received through the sensors, in addition to the acceleration data, the average heart rate is considered in the formula for calculating calories. The user enters his/her weight, gender, age, and time, to calculate calorie. It stores the data in the database by pressing the save button. When the result button is pressed, the amount of calorie and the data stored in the database are displayed on the separate page. Moreover, the acceleration and the heart rate data are displayed graphically to the user. Figure 8 illustrates an overview of communication between the designed hardware and software. The sensor's data are transferred via Bluetooth to a smartphone in a serial and real-time manner.

Experimental Design

Photoplethysmography sensor calibration

The detected R-peaks are not always accurate. A comparator circuit along with the potentiometer was used to reduce the signal's noise. The comparator circuit compared the two voltages to indicate which is larger. The comparator was used to check whether the input has reached some predetermined

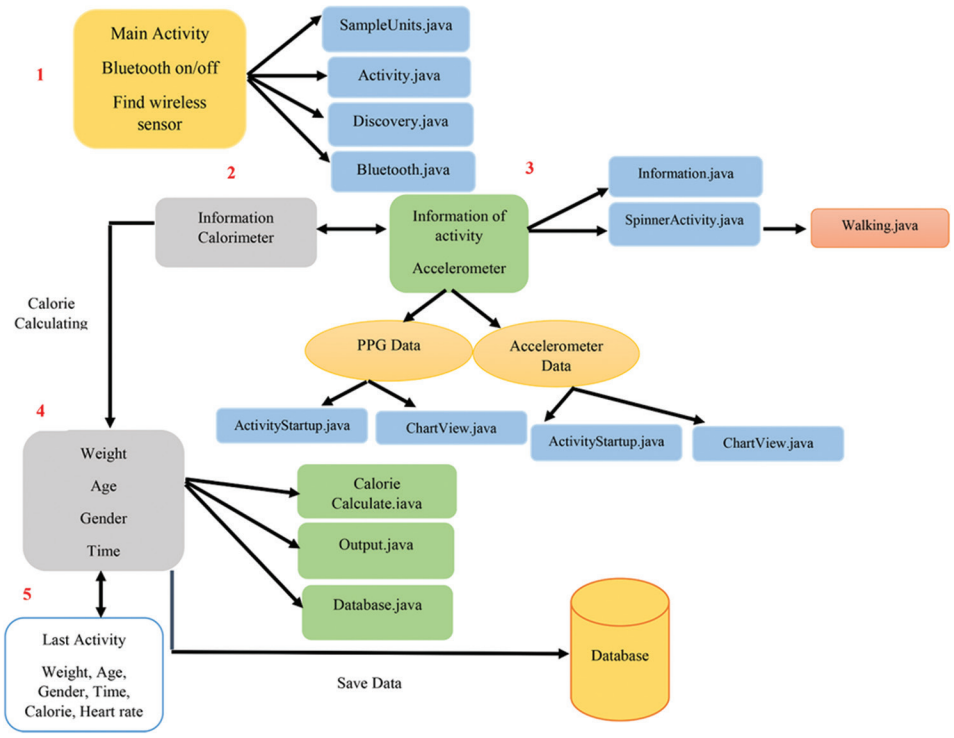

Figure 7: The communication between the application components

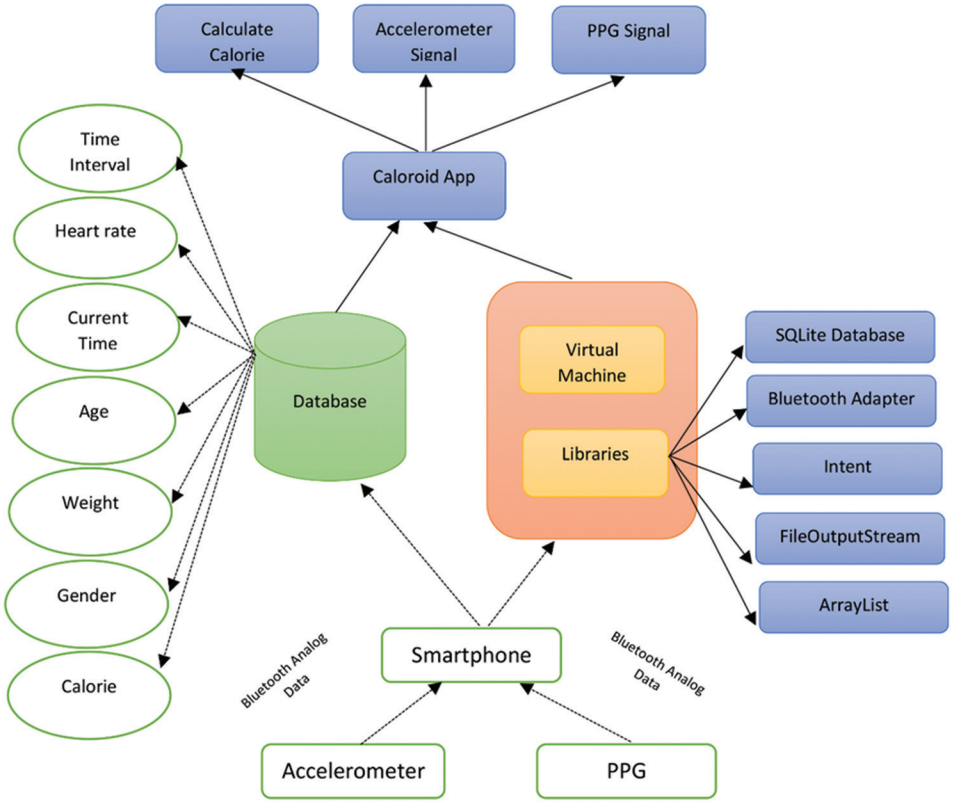

Figure 8: The overall structure of the relationship between the fitness kit's hardware and software

value. The potentiometer which is an adjustable voltage divider was used to change the negative base voltage. The potentiometer was adjusted until the number of additional pulses disappeared and the extra beats were removed. The

potentiometer with 10 Ω resistor displayed only one square pulse at the fingertip at each R-peak.

Accelerometer calibration

Before using the accelerometer, it has been calibrated with no-turn or single-point calibration. The typical orientation of a device puts the X and Y axes in a 0 g field. The accelerometer error is due to offset. It was assumed that the gain of the accelerometer is 1 and then the offset was measured. The accelerometer axis of interest was placed into a 0 g field and the output was measured. The output was equal to the offset which was subtracted from the output of the accelerometer before processing the signal.

Accelerometer filtering

The acceleration data are obtained under the three axes of X, Y and Z. To analyze the signal and eliminate the noise, the total acceleration from the three axes was calculated according to the Eq. (1).

$$a_{total} = \sqrt{x^2 + y^2 + z^2} \quad \text{Eq. (1)}$$

To eliminate the sharp spikes generated in the output acceleration signal and to suppress the noise which is out of the frequency band, the discrete wavelet transform (DWT) method was used. The Fourier analysis provides the information, localized in frequency space; however, the wavelet method retains both the frequency and the time localization. The general de-noising procedure using DWT involves three steps of decomposition, thresholding the detail coefficients, and reconstruction of the signal.[32] The process of decomposition recursively partitions complex signals into basis signals of finite bandwidth is called the analyzing wavelets or mother wavelets ψ(t). A basis function varies in scale by dividing the same function or data space using different scale sizes using scaling function ϕ(τ) (also called father wavelet) in the time domain. For example, a signal over the domain of 0–1 could be divided from 0 to ½ and ½ to 1, or it could be divided from 0 to ¼, ¼ to ½, ½ to ¾, and ¾ to 1. Each set of representations codes the original signal with a particular resolution or scale. Then, the coefficients (or weights) of these wavelets are examined. Decomposition of the signal into different frequency bands takes place, with low-pass and high-pass filters. Thus, the initial signal x[n] is passed through two filters, which are high-pass filters of g[n] and low-pass filter of h[n]. The two filters are quadrature mirror filters which satisfy the orthogonal conditions. These filters form the signal separation operation with the DWT. The output obtained from the half-band low-pass filter are the two high-pass and low-pass filter. This process continues until it reaches the desired value.[33-35]

$$Y_{high}[k] = \sum_n x[n].g[-n+2k] \quad \text{Eq. (2)}$$

$$Y_{low}[k] = \sum_n x[n].h[-n+2k] \quad \text{Eq. (3)}$$

The Eqs. (2) and (3), respectively, are related to high-pass and low-pass filter output. The corresponding operations at each level halve the number of samples. They filter and double the sampling interval, resulting in a band containing half of the frequency components. Thus, the accuracy for frequency separation is doubled.[33-35] The low-pass filter or the averaging filter removes the high-frequency fluctuations and preserves the signal's trend to preserve the approximation of the signal. However, the high-pass filter or the detail filter consists of the high-frequency fluctuations. The signal coefficients are set to zero when they are smaller than a threshold.[36] The process of decomposition is only iterated on the low-pass filter by a cascade of identical cells based on the low-pass and high-pass filters. When the signal passes through the filters, the bandwidth is halved in the down-sampling process. After the noise is removed by thresholding, the signal reconstruction process is begun by the up-sampling process. The resulting components are added together, starting from the lowest frequency component with the coarsest scale to next finer scale coefficient. Figure 9 shows the wavelet transform at the decomposition and reconstruction stage. The "h" is a low-pass filter, "g" is a high-pass filter, H_D and G_D are filters in the decomposition stage, and H_R and G_R are the filters in the reconstruction stage. The box "↓2" represents the down-sampling and the box "↑2" shows the up-sampling.[37]

Figure 10 shows the primary signal of the acceleration data and the filtered signal under the walking activity. The acceleration signal was analyzed with the five levels of the Haar wavelet filter. The Haar sequence proposed in 1909 by Haar[38] uses the analysis of signals with sudden transitions. The Haar wavelet is a step function with mother wavelet taking values 1 and −1, on [0, 1/2) and [1/2, 1), respectively. The Haar scaling function φ(t) is unity on the interval [0, 1). By changing the threshold in each level, the best-filtered signal is obtained.[39] Figure 11 shows the filtered signal and the original signal of the acceleration

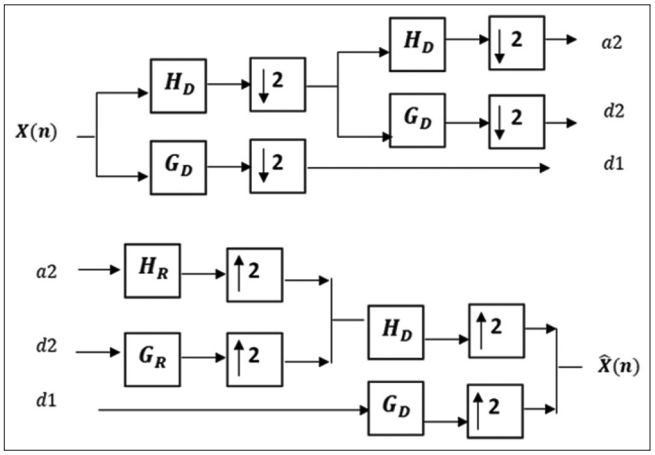

Figure 9: The discrete wavelet transform filtering using the wavelet decomposition tree and the signal reconstruction

data under the running activity. The original signal is in red and the filtered signal is in violet. Regarding the shape, the number of spike peaks in the filtered signal is reduced compared with that of the original signal. The threshold coefficients for level 1, 2, 3, 4, and 5 were considered 6.41, 7.04, 4.52, 3.20, and 2.36, respectively. At each level, when the signal analysis was carried out, the signal spectrum was examined. By changing the wavelet transform coefficients, the most suitable filtered signal was extracted from the specified range.

The variance of the acceleration signal during a single-user walking activity before filtering was 3.2. However, by applying the wavelet filter, the variance of the acceleration signal was reduced to 0.82 [Figure 10]. Similarly, the variance of the acceleration signal during a single-user running activity before filtering was 3. However, by applying the wavelet filter, the variance of the acceleration signal was reduced to 0.9 [Figure 11].

After the filtering process, 20 nonathlete subjects were randomly selected, between the age of 20 and 29 with an equal number of male and female. The two activities of running and walking were considered in terms of the average acceleration, variance, and standard deviation. According to Table 2, during the walking activity (W), the average acceleration was 9.17 m/s^2 with the average variance of 0.62 and the average standard deviation of 0.74. During the running activity (R), the average acceleration was 9.67 m/s^2 with the average variance of 0.61 and the average standard deviation of 0.79.

Table 2: The statistical data for walking and running activity after filtering the accelerometer data

User	Mean_W	Variance_W	SD_W	Mean_R	Variance_R	SD_R
1	9.75	0.60	0.80	9.72	0.62	0.70
2	9.60	0.55	0.70	9.63	0.58	0.76
3	9.73	0.68	0.80	9.71	0.66	0.8
4	9.70	0.60	0.77	9.73	0.62	0.78
5	9.60	0.50	0.70	9.64	0.54	0.73
6	9.72	0.52	0.72	9.72	0.58	0.76
7	9.36	0.58	0.76	9.34	0.72	0.84
8	9.56	0.54	0.73	9.54	0.54	0.73
9	9.87	0.66	0.81	9.72	0.68	0.82
10	9.9	0.64	0.80	9.78	0.65	0.8
11	9.45	0.62	0.78	9.62	0.54	0.73
12	9.43	0.67	0.81	9.54	0.66	0.80
13	9.7	0.58	0.76	9.75	0.59	0.76
14	9.72	0.62	0.78	9.82	0.68	0.82
15	9.67	0.64	0.80	9.78	0.63	0.79
16	9.57	0.70	0.83	9.71	0.75	0.86
17	9.6	0.68	0.82	9.65	0.67	0.81
18	9.40	0.65	0.80	9.72	0.72	0.84
19	9.40	0.67	0.81	9.54	0.65	0.80
20	9.70	0.70	0.83	9.76	0.73	0.85

SD – Standard deviation

Therefore, wavelet filtering has reduced the scattering of data and has removed the sharp spike noises from the accelerometer the output data.

Calorie consumption using the heart rate

The present mHealth App takes advantage of the heart rate and the accelerometer data to measure the calorie consumption. An Android App was designed to calculate how much calories are consumed based on the acceleration and the heart rate data [Figure 12]. The simultaneous use of two data types can increase the calculation accuracy. The

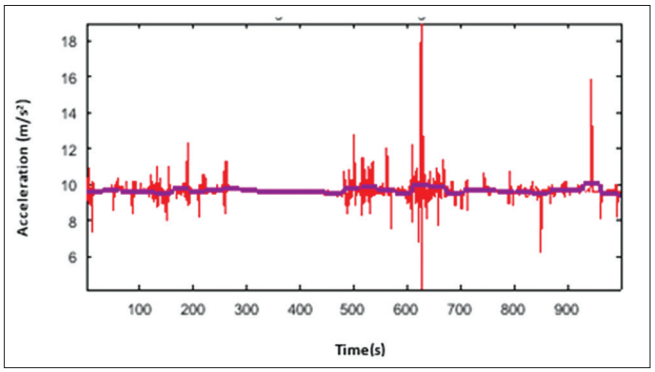

Figure 10: The original signal (in red) and the filtered signal user

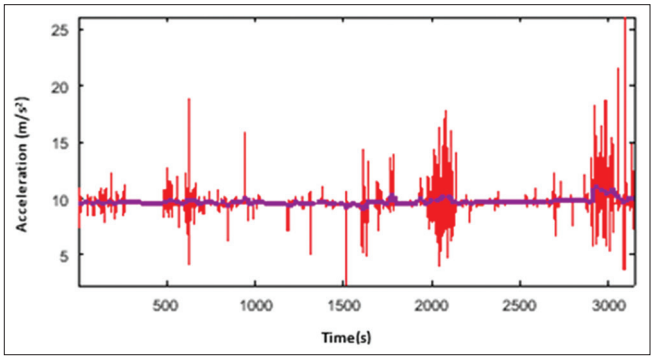

Figure 11: The original signal (in red) and the filtered signal (in purple) from the running activity of a single user

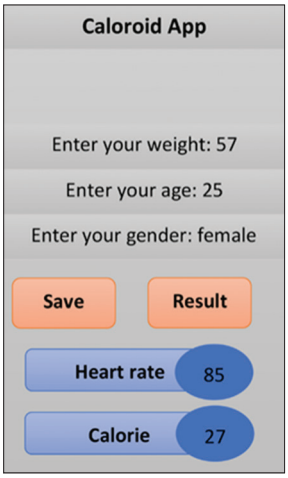

Figure 12: The input screen to calculate the calorie and the heart rate

smartphone App can determine the calorie consumption according to the user's gender. The Eq. (4) is used for female and Eq. (5) is used for male.[40] After the serial data are transmitted via the Bluetooth to the App, a number of parameters including gender, age, weight, and time may be considered in the calculation. The input and the output data are stored in a database along with a timestamp and can be accessed by the user.

$$\left(\begin{array}{c}\left(-20.4022+\left(0.4472\times H\right)-\left(0.1263\times W\right)\right)\\ +\left(0.074\times A\right)/4.184\end{array}\right)\times 60\times T \quad \text{Eq. (4)}$$

$$\left(\begin{array}{c}\left(-55.0969+\left(0.6309\times H\right)+\left(0.1988\times W\right)\right)\\ +\left(0.2017\times A\right)\end{array}\right)/4.184\times 60\times T$$

Eq. (5)

Where *H*, *T*, *A*, and *W* denote the heart rate, time, age, and weight, respectively. The coefficients shown in this formula are obtained empirically from the literature.[40-42]

Calorie consumption using the acceleration sensor

In addition to the heart rate, the acceleration data were used to calculate the calorie consumption. The primary objective is to calculate the calories using the energy from the Newtown's second law. According to Eq. (6), the necessary parameters are the number of steps, step length, weight, and acceleration. Using Newton's second law, i.e., F = ma, the person's force is calculated.

$$\vec{E}=\int F.\overrightarrow{dr}=\int ma.\overrightarrow{dr}=m\int \vec{a}.\overrightarrow{dr}=m.\sum \overrightarrow{a_i}.\overrightarrow{dr_i}=m.\overrightarrow{dr_i}.\sum \overrightarrow{a_i}$$

Eq. (6)

The *dr* represents the distance which includes the number of steps and step length. It is calculated as the product of the two components. The *dr* is a multiplication of *n* and l, which *n* is the count of steps and l is the length of steps. By analyzing the acceleration data from the uniform movement, using the Eq. (6), one can calculate the consumed calories. The calculations were carried out on the smartphone App. Therefore, in this design, both the hardware and the Android software were combined to obtain the related health data. Figure 13 depicts the print screen which takes the weight as an input. The screen shows the user's calorie consumption and the heart rate while walking. The output data are stored in the database to be retrieved in the future.

Results

Population

The accelerometer and the PPG sensors are mounted on the ankle and the finger in the form of a kit. The user receives the output analysis instantaneously on the mobile App. Figure 14 illustrates the kit mounted on the ankle and the finger for the assessed volunteer.

First, our device validity and reliability were examined by comparing it with a typical smart band, smart watch, and smartphone available in the market. At this stage, only three individuals were used as our population. User 1 was a 28-year-old female with the 67 kg weight, 161 cm height, and body mass index (BMI) of 25.8. User 2 was a 29-year-old female with the 54 kg weight, 150 cm height, and BMI of 24.0. User 3 was a 26-year-old female with the 56 kg weight, 158 cm height, and BMI of 22.4. To compare our proposed device functionality with the commercial mobile devices, a Huawei smart watch, a Mi-Band smart band, and a Galaxy S7 smartphone were used to calculate the step count, calorie consumption, and heart rate. Five different activities of walking, running, standing, sitting, and sleeping have been investigated. An observer was assigned to count the actual number of steps as a benchmark to compare the four different devices' step count and calorie consumption. The commercial pulse oximeter device was used to measure the actual heart rate. Each activity lasted for a period of 6 min. All three users were tested under the same environmental conditions. In this experiment, the

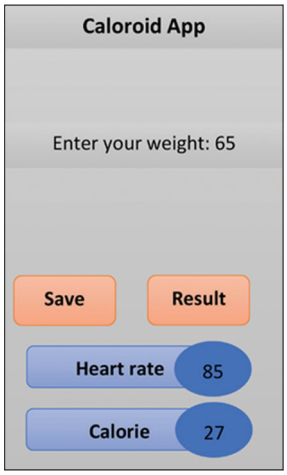

Figure 13: The calorie consumption calculation using the acceleration data

Figure 14: The sensor mounted on the finger and ankle

smart watch was worn on the left wrist, the smart band was placed on the right wrist, the smartphone was placed on the palm facing up, and the proposed device was mounted on the ankle and finger. Results are presented below.

Next, the 20 individuals were selected randomly in an equal number of male and female, aged 25–63, with the weight of 45–95 kg, and with the height of 150–178 cm. All of the participants were healthy and nonathletes. The individuals walked under identical conditions and receive real-time data of heartbeat rate and consumed calorie. Then, our device validity and reliability were compared with the pulse oximeter, which is the gold standard for the PPG sensor, and the treadmill which is the gold standard for the accelerometer as follows:

- The correlation of calorie consumption in PPG and pulse oximeter
- The correlation of calorie consumption in accelerometer and treadmill.

Finally, the correlation of calorie consumption with gender, age, and weight was examined on the population when using the PPG and the accelerometer sensors.

Statistical analysis

A hypothesis test is performed to determine the significance of the result and to test our claim about the validity and reliability of the designed PPG/accelerometer kit by a *P* value. Our proposed kit's output was compared with the pulse oximeter and treadmill which are considered as gold standards. The *alternative hypothesis* is our experiment's hypothesis if the null hypothesis is concluded to be untrue. The *P* value is a number between 0 and 1 and weighs the strength of the evidence and interpreted in the following way:

- A small *P* value (typically ≤0.05) indicates the alternative hypothesis is true and the null hypothesis is rejected
- A large *P* value (>0.05) indicates the alternative hypothesis is not true and the null hypothesis is failed to be rejected.

Next, the root mean square error (RMSE) is calculated which is the standard deviation of the residuals (prediction errors) and how much spread out these residuals are. In other words, it indicates how concentrated the data from the designed device are around the data obtained from the gold standard devices. In Eq. (7), the *x* variable is calorie consumption of PPG and accelerometer and *y* variable is the calorie consumption from the pulse oximeter and treadmill.

$$\mathrm{RMSE}=\sqrt{\frac{\sum_{i=1}^{N}\left(x(i)-y(i)\right)^2}{N-1}} \qquad \text{Eq. (7)}$$

The correlation of calorie consumption with gender, age, and weight was obtained by the Pearson's product-moment correlation. It is used since the samples from the sensors are numerical values. The *r* value is the Pearson correlation coefficients. The Pearson's product-moment correlation measures the strength of the linear association between the two numeric variables *x* and *y*. The correlation (*r*) is a unit-less quantity, where:[41]

- $-1 \le r \le 1$
- If $r < 0$, then there is a negative association between *x* and *y*, i.e., as *x* increases, *y* generally decreases
- If $r > 0$, then there is a positive association between *x* and *y*, i.e., as *x* increases, *y* generally increases
- The close *r* is to 0 the weaker the linear association between *x* and *y*.

Then, a regression equation is used to find out what relationship, if any, exists between the sets of data. In simple linear regression, it is assumed that the mean can be modeled using the function that is a linear function of unknown parameters. In linear regression, the regression line is a perfectly straight line. The regression model is *y* = mean + random scatter.

Comparison of the proposed device with the commercial devices

Here, results from the five activities of walking, running, standing, sitting, and lying are presented. Four mobile devices are compared, and the average step count error in 100 steps and the average heart rate error in 100 pulses from the three users are illustrated in Table 3. The commercial devices indicated a false number of steps and pulses, either higher or lower than the accurate measurement. For example, during the user 1's walking activity, a step count of 452 was recorded as 1027 steps by smart watch. In addition, the small movement toward the right or left direction of the smartphone, the number of steps is inaccurately multiplied, which indicates the inadequacy of the sensor inside the smartphone. Furthermore, when the users were sitting, standing, and sleeping, the smart watch, the smart band, and the smartphone indicated a step count greater than zero. However, the proposed device displays the steps count of zero for all three activities. Moreover, the measured heart rate value for user 1 in a walking mode using a smart watch, smart band, smartphone, and the proposed device was 62, 88, 78, and 84, respectively, while the actual value was 85.

Comparison of the proposed device with the gold standard devices

The output provided by the PPG and the accelerometer was compared to that of the gold standard, pulse oximeter, and treadmill, respectively. The 20 participants walked for 15 min on a flat surface of the treadmill. Figures 15 and 16 represent age versus calorie consumptions for male and females.

According to the results, there is no significant difference in the values obtained from the PPG and the pulse

Table 3: The comparison of the proposed device with the commercial devices for 3 users

Activity	Device	Average step count error in 100 steps (+) Indicates the number of the overestimated steps (−) Indicates the number of the underestimated steps	Average heart rate error in 100 pulses (+) Indicates the number of the overestimated pulse (−) Indicates the number of the underestimated pulse
Walking	Smart watch	56+	37−
Running		31+	54−
Standing		Not available	14−
Sitting		Not available	19+
Lying		Detects steps	29+
Walking	Smart band	65+	4+
Running		71+	14+
Standing		Not available	5+
Sitting		Detects steps	18+
Lying		Detects steps	23+
Walking	Smartphone	50+	3−
Running		65+	10−
Standing		Not available	4+
Sitting		Not available	8+
Lying		Not available	10+
Walking	Our device	1−	1−
Running		20+	4+
Standing		Detects no steps	2−
Sitting		Detects no Steps	3+
Lying		Detects no steps	3+

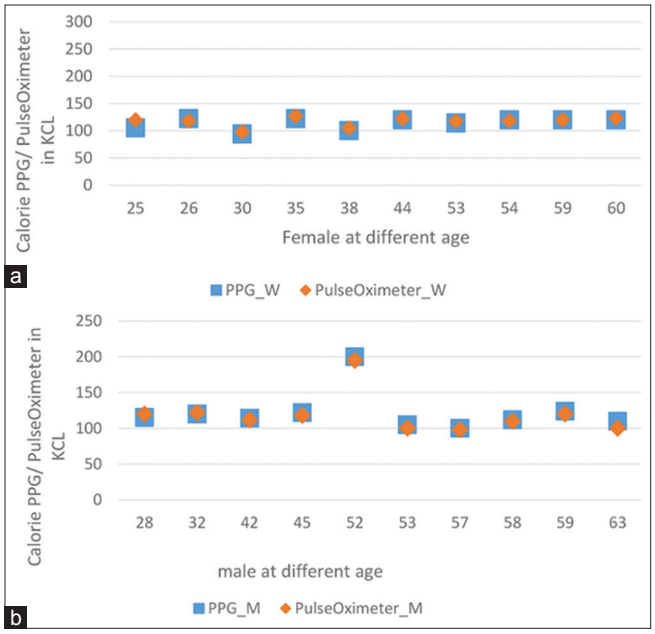

Figure 15: The calorie consumption comparison between the pulse oximeter and photoplethysmography for (a) female and (b) male

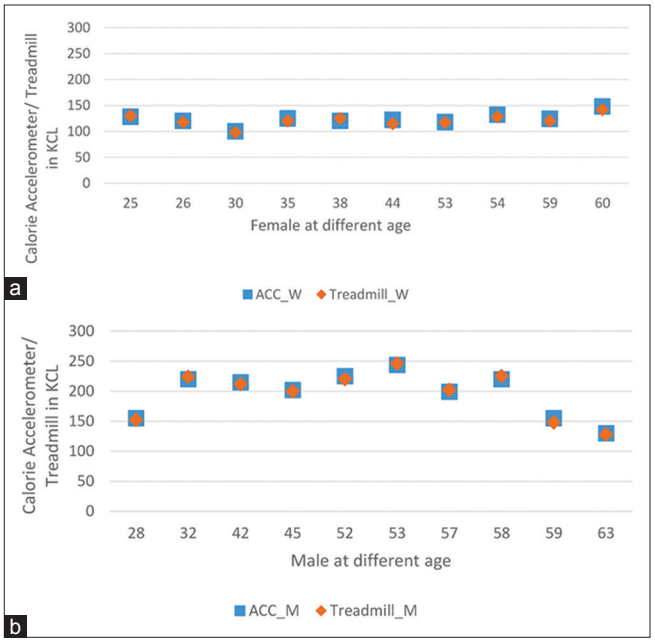

Figure 16: The calorie consumption comparison between the accelerometer and the treadmill for (a) female and (b) male

oximeter. Furthermore, similar results were obtained for the accelerometer and the treadmill. Therefore, the output from our proposed kit is aligned with the gold standard. The RMSE of calorie consumption between PPG and pulse oximeter for both female and female was 0.53 and the $P = 0.008$ ($P < 0.05$). Moreover, the RMSE of calorie consumption for both male and female between the treadmill and accelerometer was 0.4 with the $P = 0.007$ ($P < 0.05$). The correlation of PPG/pulse oximeter and accelerometer/treadmill is strong and equal to 0.9. Thus, the proposed sensors enjoy the high precision and could be considered a competitive device to the pulse oximeter and treadmill available in the market.

Calorie consumption with gender using the photoplethysmography and the accelerometer

According to Figure 17, females have consumed fewer calories during the similar activity comparing with males when measuring by the PPG sensor. Moreover, Figure 18 shows that female have consumed fewer calories than male using the accelerometer sensor. According to Figures 17 and 18, the mean difference of calorie consumption of male and female for both PPG and accelerometer is 40 and 60 kcal, respectively.

Correlation of calorie consumption with weight using the photoplethysmography sensor

Figure 19 represents the correlation of calorie consumption with weight using the PPG sensor for male and female. Figure 19a shows a correlation of 0.88 for males, and the amount of correlation in Figure 19b is 0.7 for females. The results show a high correlation with a positive association. This association means that the increase in weight could increase the consumed calorie consumption in our study. The regression equation for calorie consumption values resulting from PPG and weight parameter are expressed as $y = 2.9553x - 50.76$ and $y = 1.3987x + 111.05$, respectively, in Figure 19a and b.

Correlation of calorie consumption with weight using the accelerometer sensor

Figure 20 represents the correlation of calorie consumption with the weight using the accelerometer sensor for male and female. Figure 20a shows a correlation of 0.9 for males and Figure 20b shows an amount of 0.8 for females. The results show a high correlation with a positive association and weight gain affects the calorie consumption in our experiment. The regression equation for calorie values resulting from the accelerometer and weight parameter is expressed as $y = 5.1213x - 214.44$ and $y = 2.7071x - 11.563$, respectively, in Figure 20a and b.

Correlation of calorie consumption with age using the photoplethysmography sensor

Figure 21 represents the correlation of calorie consumption of PPG with age parameter for male and female. Figure 21a shows a correlation of 0.2 and Figure 21b shows a correlation of 0.1. The results show that there is a positive association with a low correlation and high data dispersion. This dispersion means that age has shown no effects on the calorie consumption in this research. The regression equation for the calorie consumption values resulting from PPG and age parameter are expressed as $y = 1.73x + 127.38$ and $y = 0.2979x + 175.3$, respectively, in Figure 21a and b.

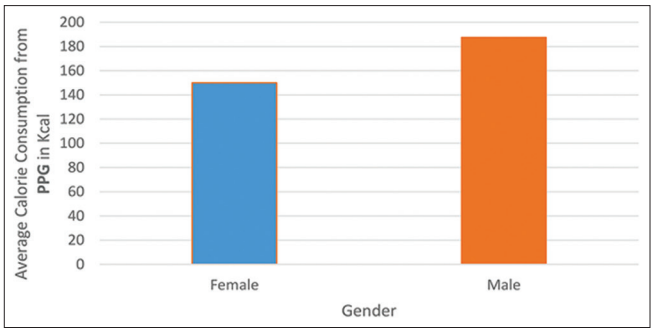

Figure 17: The relationship between the calorie consumption of photoplethysmography sensor among different gender

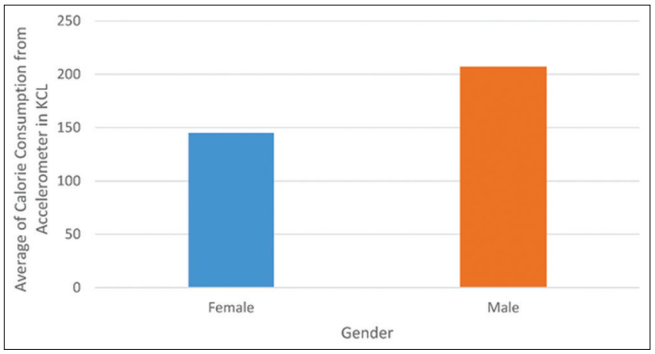

Figure 18: The relationship between the calorie consumption of accelerometer sensor among different gender

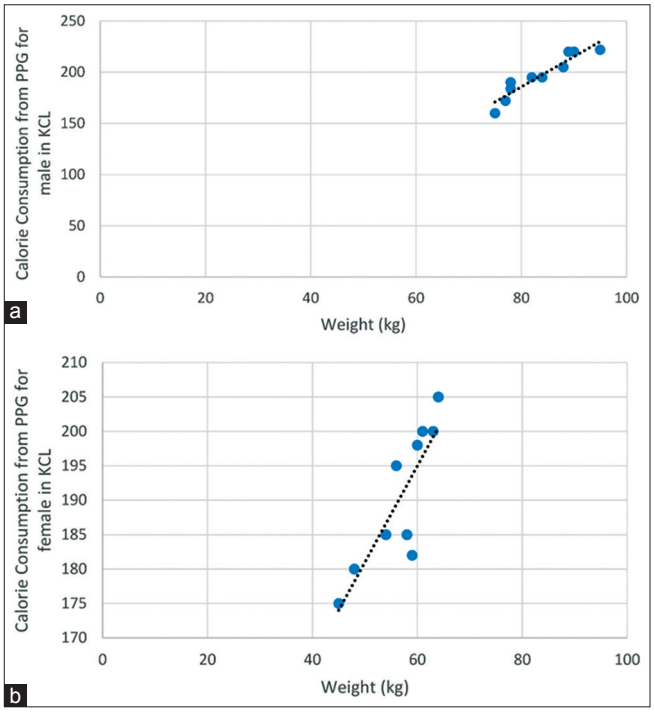

Figure 19: The correlation of calorie consumption with weight using the photoplethysmography sensor for (a) male and (b) female

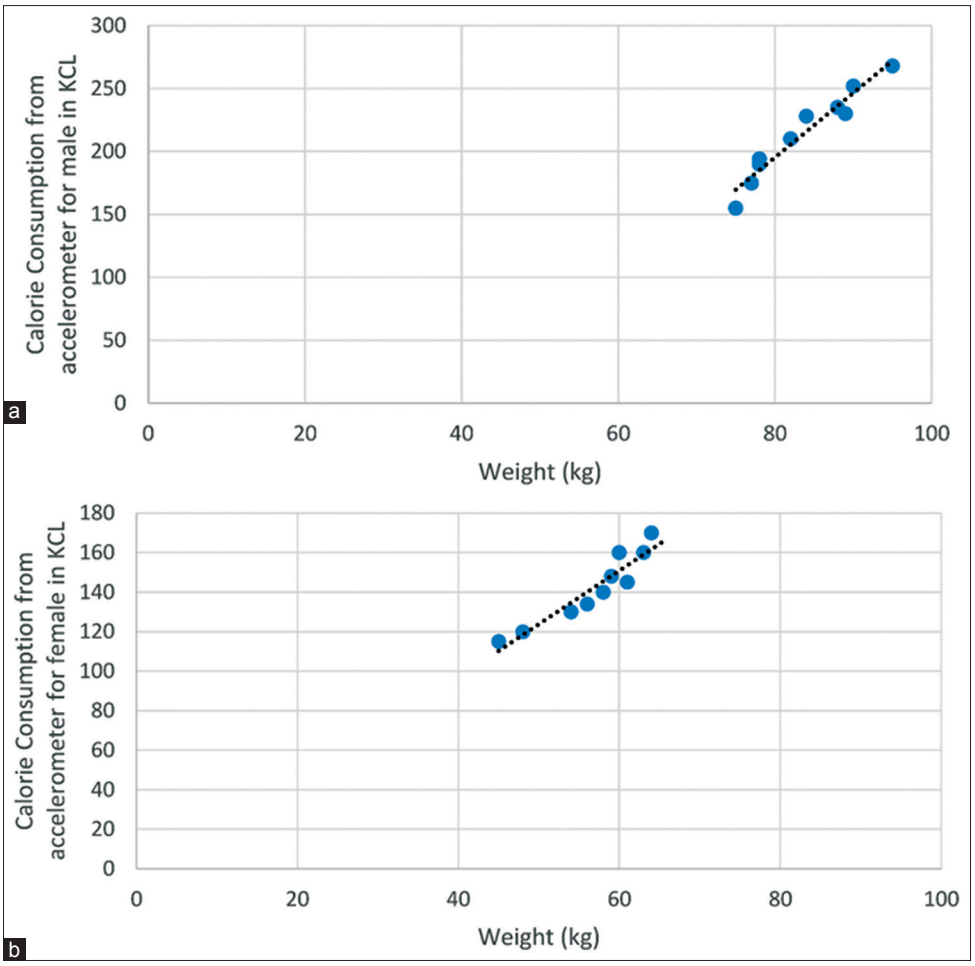

Figure 20: The correlation of calorie consumption with weight using the accelerometer sensor for (a) male and (b) female

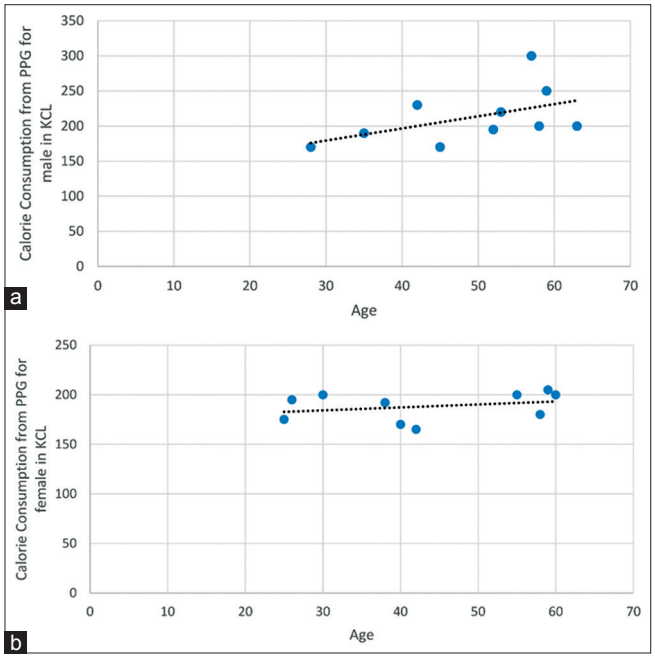

Figure 21: The correlation of calorie consumption of photoplethysmography and age parameter for (a) male and (b) female

Correlation of calorie consumption with age using the accelerometer sensor

Figure 22 represents the correlation of calorie consumption of accelerometer with the age parameter for male and female. Figure 22a shows a correlation of 0.3 for males and Figure 22b shows the correlation of 0.4 for females. The results demonstrate a low correlation with a positive association. This association means that age has shown no effects on the calorie consumption in this research. The regression equation for calorie consumption resulting from the accelerometer and age parameter are expressed as $y = 2.082x + 143.06$ and $y = 3.0466x + 65.783$, respectively, in Figure 22a and b.

Discussion

In this research, the accelerometer and PPG sensors are mounted on the ankle and finger having been connected to a smartphone App forming a fitness App to measure the user's calorie consumption. Two main improvements have been achieved compared with the previous research. (1) The PPG circuit has been improved to produce a suitable heart rate

output. The extra beats were removed using a comparator circuit in the calibration stage. (2) The accelerometer output has been improved with the single-point calibration and placing each axis into a 0 g and subtracting the offset. The sharp spikes have been removed using the DWT with five-level Haar wavelet. The filtering step retained both the frequency and time localization by the three steps of decomposition, thresholding, and reconstruction.

The validity and reliability of the proposed kit were examined by comparing it with the three commercial mobile devices available in the market. The average step count error and the average heart rate error have been examined during the five activities of walking, running, standing, sitting, and sleeping. The results are summarized in Table 4. Our proposed device output the lowest error, due to proper filtering of the noise. Only our device detects no steps while the user is carrying a sedentary action, this is due to the correct calibration of the accelerometer sensor. The smart band's accelerometer is the weakest and outputs the highest error. Our device has the lowest heart rate error, even when the user is engaged with the running activity which is device distortion is very high. The smartphone outputs the next best result because the user has tighter contact with the PPG sensor. The movement in running activity disturbs the output of the commercial device.

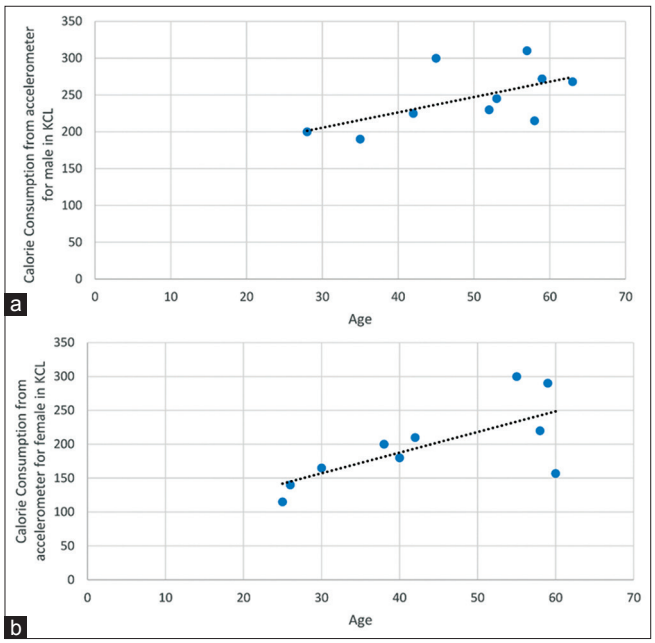

Figure 22: The correlation of calorie consumption of the accelerometer and the age parameter for (a) male and (b) female

At the next stage, the validity and reliability of our device were further examined by comparing the PPG sensor and the accelerometer sensor with the gold pulse oximeter and treadmill, respectively. According to Table 5, the RMSE of calorie consumption between the PPG and the pulse oximeter is 0.53 and the $P = 0.008$ ($P < 0.05$). Moreover, the RMSE of calorie consumption between treadmill outputs versus accelerometer is 0.42 and the $P = 0.007$ ($P < 0.05$). Furthermore, the correlation between PPG and pulse oximeter and between accelerometer and treadmill is 0.9. Therefore, there is no significant difference between the implemented devices and the gold standard.

When using both the PPG and the accelerometer devices, female burns fewer calories than male. There is a good correlation between the calorie consumption of the PPG, accelerometer sensors, and weight parameter. The weight parameter has a positive effect on the calorie consumption. There was no correlation detected between the energy expenditure on different ages.

Conclusions

In this research, a real-time mobile fitness kit is developed and evaluated. The kit consists of the PPG sensor on the finger, the accelerometer sensor on the ankle, and the smartphone tracking App. The sensors measure the heart rate and the acceleration as input to calculate the calorie consumption. Our proposed device measures the heart rate at the arterial vessel at the tip of the forefinger and could keep up with the fast pulsations. In this project, the heart rate is measured using the IR signals obtained from the PPG sensor through the index finger. The IR diode transmits an IR light into the fingertip; a photodiode based on the blood volume senses the light reflected back. The blood volume fluctuates according to the heartbeat. The calibration and wavelet filtering are applied to obtain the suitable output signal. By applying the wavelet filter, the variance of the acceleration signal was reduced considerably. Our proposed kit was evaluated against the gold standards, and the high correlation exists in PPG/pulse oximeter and accelerometer/treadmill values. Therefore, our proposed kit has the necessary accuracy to be replaced with the heavy, stationary, and expensive gold standard devices in the daily fitness-tracking activities. Then, the kit was compared with the healthcare tracking devices available on the market, namely a smartphone, a smart band, and a smart watch. The

Table 4: The average error in our device compared with the commercial devices

Activity	Average step count error in 100 steps	Average heart rate error in 100 pulses
Walking	Our device < smartphone < smart watch < smart band	Our device < smartphone < smart band < smart watch
Running	Our device < smart watch < smartphone < smart band	Our device < smartphone < smart band < smart watch
Standing	Only our device correctly detects no steps	Our device < smartphone < smart band < smart watch
Sitting	Only our device correctly detects no steps	Our device < smartphone < smart band < smart watch
Lying	Only our device correctly detects no steps	Our device < smartphone < smart band < smart watch

Table 5: The analysis of the *P* value, root mean square error, and correlation for photoplethysmography, pulse oximeter, accelerometer, Treadmill

Device and parameter	*P*	RMSE value	Correlation
PPG and pulse oximeter	0.008	0.32	0.90
Accelerometer and treadmill	0.007	0.43	0.90

RMSE – Root mean square error; PPG – Photoplethysmography

market devices do not provide an open source platform, cannot be customized, are less accurate, do not differentiate between different kinds of activities, and are very expensive. The classification of activities not only leads to the assessment of energy expenditure but also could reduce sedentary behavior and assist on early diagnosis and monitoring of psychiatric diseases, neurodegenerative diseases such as Parkinson's, Alzheimer's, and Huntington's diseases or to be used in a physical rehabilitation system for stroke patients or athletes. The market health trackers such as smart watches and smart bands that read the slow-pumping capillaries on the wrist instead of fingertip are less accurate in calculating the heartbeat. They only function at 70–80 bpm when the person is at a resting position. They employ optical sensors that have trouble tracking the heart rate in quick pulsations. Smart bands and smart watches are only accurate to measure the heart rate during the rest. Therefore, they are not useful for people with the heart disease conditions that require constant monitoring. However, our proposed kit is more accurate, possesses the activity recognition capability, has an open source platform, and costs very low price. Therefore, the present kit could be regarded as an improvement comparing to the smart health-tracking devices on the market. At the next stage of the project, the kit was used to measure the energy expenditure considering the effect of the gender, weight, and age. There was no correlation between the energy expenditure with age; however, certain amount of correlation was detected regarding weight and gender. The device implemented in this article measures the heart rate and the total acceleration instantaneously and accurately; it could replace the gold standard devices on the laboratory and the common fitness-tracking kits on the market.

Weakness and future work

This article focused on global body motion activity recognition with a single accelerometer using thresholding-based techniques to differentiate between the motion-type activities (i.e., walking and running) and the motionless activities (i.e., standing and sitting). In the future, multiple orientation-based sensors with different body placement will be used on legs and arms or body extremities such as wrists or embedded in shoes. The multiple sensors will facilitate the broader range of activity recognition. The range of activities could include daily activities such as eating, drinking, brushing, washing, and writing to exercise activities such as stretching, bicycling, climbing, weightlifting, cross-training, rowing, or swimming. This process requires various classification algorithms such as decision tree, support vector machine, or Hidden–Markov model to classify a variety of activities accurately. More refined learning algorithms such as deep learning approaches could be incorporated to address the classification problem and improve the accuracy of activity recognition.

Financial support and sponsorship

None.

Conflicts of interest

There are no conflicts of interest.

References

1. Adibi S, editor. Mobile Health: A Technology Road Map. Springer Series in Bio/Neuroinformatics. Springer International Publishing Switzerland; 2015. ISBN10: 3319128167. DOI 10.1007/978-3-319-12817-7.
2. Pettey C. Wearables Hold the Key to Connected Health Monitoring. Digital Business; 2018. Available from: https://www.gartner.com/smarterwithgartner/wearables-hold-the-key-to-connected-health-monitoring/. [Last accessed on 2018 Jul 22].
3. Fan X, Huang H, Qi S, Luo X, Zeng J, Xie Q, *et al*. Sensing home: A cost-effective design for smart home via heterogeneous wireless networks. Sensors (Basel) 2015;15:30270-92.
4. Sukaphat S. An Applying of Accelerometer in Android Platform for Controlling Weight. Nagoya, Japan: International Conference on Information and Social Science; 2013. p. 294-303.
5. Kashi S, Reddy C, Reddy AP. Fit assist step count and calorie estimator using accelerometer. Int J Adv Res Computer Commu Eng 2014;3:7912-7.
6. Gusenbauer D, Isert C, and Krösche J. Self-Contained Indoor Positioning on Off-The-Shelf Mobile Devices. Zurich: International Conference on Indoor Positioning and Indoor Navigation; 2010. p. 1-9.
7. Hwang P, Chou C, Fang W, Hwang C. Smart Shoes Design with Embedded Monitoring Electronics System for Healthcare and Fitness Applications. Nantou: IEEE International Conference on Consumer Electronics-Taiwan (ICCE-TW); 2016. p. 1-2.
8. Adi E, Joko P, Yeh C, Chou N, Lee M, Lin AY. Integrated wearable system for monitoring heart rate and step during physical activity. Mob Inf Syst 2016;2016:10.
9. Pande A, Zhu J, Das AK, Zeng Y, Mohapatra P, Han JJ. Using smartphone sensors for improving energy expenditure estimation. IEEE J Transl Eng Health Med 2015;3:2700212.
10. Pal BS, Hepsiba D. Real-time monitoring of daily calorie expenditure using smart phone. Int J Adv Res Comput Sci Softw Eng 2013;3:268-73.
11. Duclos M, Fleury G, Lacomme P, Phan R, Ren L, Rousset S. An acceleration vector variance-based method for energy expenditure estimation in a real-life environment with a smartphone/smartwatch integration. Expert Syst Appl 2016;63:435-49.
12. Li M, Kwak KC, Kim YT. Estimation of energy expenditure using a patch-type sensor module with an incremental radial basis function neural network. Sensors (Basel) 2016;16. pii: E1566.
13. Altini M, Penders J, Vullers R, Amft O. Estimating energy expenditure using body-worn accelerometers: A comparison of methods, sensors number and positioning. IEEE J Biomed Health Inform 2015;19:219-26.
14. Carneiro S, Silva J, Aguiar B, Rocha T. Accelerometer-Based Methods for Energy Expenditure using the Smartphone. Turin: IEEE International Symposium on Medical Measurements and

Applications (MeMeA) Proceedings; 2015. p. 151-6.
15. Boman M, Sanches P. Sensemaking in intelligent health data analytics. KI Künstliche Intell 2015;29:143-52.
16. Duus R., Cooray M, Page N. Agentic technology: The impact of activity trackers on user behavior (an extended abstract). In: Stieler M, editors. Creating Marketing Magic and Innovative Future Marketing Trends. Developments in Marketing Science: Proceedings of the Academy of Marketing Science. Cham: Springer; 2017. p. 315-22.
17. Asimina S, Chapizanis D, Karakitsios S, Kontoroupis P, Asimakopoulos DN, Maggos T, *et al*. Assessing and enhancing the utility of low-cost activity and location sensors for exposure studies. Environ Monit Assess 2018;190:155.
18. Camp CM, Hayes LB. Identifying beneficial physical activity during school recess: Utility and feasibility of the fitbit. J Behav Educ 2017;26:394-409.
19. Schneider M, Chau L. Validation of the fitbit zip for monitoring physical activity among free-living adolescents. BMC Res Notes 2016;9:448.
20. Hamari L, Kullberg T, Ruohonen J, Heinonen OJ, Díaz-Rodríguez N, Lilius J, *et al*. Physical activity among children: Objective measurements using fitbit one® and ActiGraph. BMC Res Notes 2017;10:161.
21. King CE, Sarrafzadeh M. A survey of smartwatches in remote health monitoring. J Healthc Inform Res 2018;2:1-24.
22. Boletsis C, McCallum S, Landmark BF. The use of smartwatches for health monitoring in home-based dementia care. In: Zhou J, Salvendy G, editors. Human Aspects of IT for the Aged Population. Design for Everyday Life. Lecture Notes in Computer Science. Vol. 9194. Cham, Springer: Springer; 2015. p. 15-26.
23. Bojanovsky V, Byrne S, Kirwan P, Cleland I, Nugent C. Evaluation of fall and seizure detection with smartphone and smartwatch devices. In: Ochoa S, Singh P, Bravo J, editors. Ubiquitous Computing and Ambient Intelligence. Lecture Notes in Computer Science. Vol. 10586. Cham: Springer; 2017. p. 275-86.
24. Capodieci A, Budner P, Eirich J, Gloor P, Mainetti L. Dynamically adapting the environment for elderly people through smartwatch-based mood detection. In: Grippa F, Leitão J, Gluesing J, Riopelle K, Gloor P, editors. Collaborative Innovation Networks. Studies on Entrepreneurship, Structural Change and Industrial Dynamics. Cham: Springer; 2018. p. 65-73.
25. Fit Bit Official Website; 2018. Available from: https://www.fitbit.com/flex2. [Last accessed on 2018 Aug 18].
26. Garmin Vivofit Official Website; 2018; Available from: https://www.activestride.com.au/garmin-vivofit-replacement-bands. [Last accessed on 2018 Aug 18].
27. Huawei Website; 2018. Available from: https://consumer.huawei.com/us/wearables/watch/. [Last accessed on 2018 Aug 18].
28. Apple Website; 2018. Available from: https://www.apple.com/shop/buy-watch/apple-watch. [Last accessed on 2018 Aug 18].
29. Swain DP, Abernathy KS, Smith CS, Lee SJ, Bunn SA. Target heart rates for the development of cardiorespiratory fitness. Med Sci Sports Exerc 1994;26:112-6.
30. Kim JW, Park C. A step stride and heading determination for the pedestrian navigation system. J Glob Positioning Syst 2004;3:273-9.
31. The ADXL335 Accelerometer Datasheet. Available from: https://www.sparkfun.com/datasheets/Components/SMD/adxl335.pdf. [Last accessed on 2018 May 04].
32. Chiu CK. An Introduction to Wavelets: Academic Press, Harcourt Brace Jovanovich; 1992. p. 266.
33. Daubechies I. Ten Lectures on Wavelets. J Acoust Soc Am 1992. p. 357.
34. Hernandez E, Weiss GL. A First Course on Wavelets. Studies in Advance Mathematics: CRC Press Inc.; 1996. p. 489.
35. Unser M, Aldroubi A. A review of wavelets in biomedical applications. Proc IEEE 1996;84:626-38.
36. Donoho DL. Denoising by soft-thresholdin. IEEE Trans Inf Theory 1995;41:613-27.
37. German-Sallo Z, Ciufudean C. Waveform adapted wavelet denoising of ECG signals. Proceedings of the 14th WSEAS International Conference on Mathematical and Computational Methods in Science and Engineering (MACMESE '12). Sliema, Malta; Adv Math Comput Methods 2012. p. 172-5.
38. Haar A. On the theory of orthogonal functions systems. Doctorate thesis, University of Gottingen, Germany; 1909.
39. Strang G. Wavelets. Am Sci 1992;82:250-5.
40. Keytel LR, Goedecke JH, Noakes TD, Hiiloskorpi H, Laukkanen R, van der Merwe L, *et al*. Prediction of energy expenditure from heart rate monitoring during submaximal exercise. J Sports Sci 2005;23:289-97.
41. Ceaser TG. The Estimation of Caloric Expenditure Using Three Triaxial Accelerometers. Ph.D. Dissertation. University of Tennessee; 2012.
42. Uri D, Mayette GG. Evaluating a Novel Device for Calorie Reduction: The Bite Counter Study. Open Access Master's Theses; 2016. p. 895. Available from: http://digitalcommons.uri.edu/theses/895. [Last accessed on 2019 Sep 22].

BIOGRAPHIES

Faranak Fotouhi-Ghazvini received her MEng degree in Telecommunication Engineering from King's College London (UK) in 2001 (1st class), and her PhD degree from Bradford University (UK), Department of Informatics in 2011. She is an Assistant professor at Department of Computer Engineering and Information Technology and the director of IoT and Smart Environments Research Group in University of Qom. Her research interests include Internet of Everything (IOT), Wearable Computing and Deep Learning.

Email: f-fotouhi@qom.ac.ir

Saedeh Abbaspour she has received her master degree in Information Technology in 2015. She is currently a PhD student at Department of Computer Engineering and IT, University of Qom, Iran. Her research interests include Internet of Everything (IOT), Wearable Computing and Deep Learning.

Email: saedeh.abbaspour@gmail.com